Downloaded from http://jgs.lyellcollection.org/ at Massachusetts Institute of Technology on September 17, 2019

Journal of the Geological Society, London, Vol. **162**, 2005, pp. 373–388. Printed in Great Britain.

Transcurrent shearing, granite sheeting and the incremental construction of the tabular 3.1 Ga Mpuluzi batholith, Barberton granite–greenstone terrane, South Africa

JANUS D. WESTRAAT[1], ALEXANDER F. M. KISTERS[1], MARC POUJOL[2] & GARY STEVENS[1]

[1]*Department of Geology, University of Stellenbosch, Private Bag X1, Matieland 7602, South Africa (e-mail: akisters@sun.ac.za)*

[2]*Department of Earth Sciences, Memorial University of Newfoundland, St. John's, Nfld., A1B 3X5, Canada*

Abstract: Structural, petrographic and geochronological studies show that the tabular 3.1 Ga Mpuluzi batholith in the Barberton granite–gneiss terrane in South Africa was emplaced via a combination of external and internal processes. External structural controls are indicated by systematic variations in intrusive relationships and strain along the margins of the Mpuluzi batholith and are consistent with an emplacement of the granite in a dilational jog within a NE–ENE-trending system of dextral transcurrent synmagmatic shear zones. Internally, the Mpuluzi batholith is essentially made up of granite sheets. The structurally higher parts of the granite are made up of shallowly dipping sheets that are underlain by an anastomosing network of steeply dipping, variably deformed dykes and sheets. These granite sheets at lower structural levels intruded either into the actively deforming shear zones or into extensional sectors between and along the bounding shear zones. Multiple intrusive relationships and geochronological evidence suggests that granite sheeting and the assembly of the pluton occurred over a period of 3–13 Ma. The spatial and temporal relationship between deformation and magma emplacement reflects episodes of incremental dilation related to deformation along the bounding shear zones and granite sheeting. The transition to the mainly subhorizontal granite sheets at higher structural levels of the tabular Mpuluzi batholith indicates the intrusion of the granites during subhorizontal regional shortening, where the reorientation of the minimum normal stress to vertical attitudes at the shallow levels of emplacement allowed for vertical dilation and subhorizontal emplacement of the granite sheets.

Keywords: Archaean, Mpuluzi batholith, granites, shear zones, absolute age.

The petrogenesis of granites is almost invariably linked to active orogenic settings and the transport and emplacement of granitic magmas is now widely recognized to be aided and/or controlled by regional-scale structures such as fault and shear zones, fold structures or regional fabric patterns (e.g. Hutton 1988; Paterson & Fowler 1993; Collins & Sawyer 1996; Clemens *et al*. 1997; Petford *et al*. 2000). The intrusion of granitoids along and into actively deforming wall rocks presents an elegant solution to the so-called space problem of granite emplacement in that deformation potentially creates regions of localized dilation in a variety of kinematic scenarios, including extensional, convergent and wrench-tectonic environments (e.g. Guineberteau *et al*. 1987; Hutton & Ingram 1992; Tikoff & Teyssier 1992; Vauchez *et al*. 1997; Brown & Solar 1998). One of the most widely used approaches to decipher the actual mechanisms of granite emplacement is the structural analysis of wall-rock strains in the strain aureole of granites and within the granites themselves (Paterson *et al*. 1989; Ramsay 1989). However, a distinction between regional strains related to, for example, shear zones or regional foliation patterns that may have controlled granite emplacement, and emplacement-related strains caused by the granitoids themselves, such as granite ballooning and the displacement of wall rocks, is commonly difficult (Cruden 1998). In both cases, the superimposition of regional and intrusion-induced strains is common, and granite emplacement is, in most cases, achieved through multiple mechanisms that can be both of a regional and a more local nature (Paterson & Fowler 1993).

By far the most prolific period of granite production and crustal differentiation was the Archaean, when significant parts of the present continents were formed during accretionary tectonic events and associated short-lived but voluminous episodes of granitoid magmatism. The actual nature of events that prompted the production of these vast amounts of granitoids is as ambiguous and controversial as the modes of emplacement of the granitoid magmas. It is, thus, not surprising that Archaean cratons and their granite–greenstone terranes have often been at the centre of the debate about granite ascent and emplacement mechanisms (e.g. Ramsay 1989; Jelsma *et al*. 1993; Ridley *et al*. 1997; Van Kranendonk *et al*. 2004). The Palaeo- to Mesoarchaean Barberton granite–greenstone terrane in the Kaapvaal Craton in South Africa (Fig. 1) has featured very prominently in this debate (Viljoen & Viljoen 1969; Anhaeusser 1973; De Wit *et al*. 1992). This composite granite–greenstone terrane was assembled during several tectonomagmatic episodes between *c*. 3.5 and 3.1 Ga (e.g. Anhaeusser & Robb 1980; Robb & Anhaeusser 1983; Armstrong *et al*. 1990; De Ronde & De Wit 1994; Kamo & Davis 1994). Earlier, *c*. 3.5–3.2 Ga plutonic suites are characterized by trondhjemites, tonalites and granodiorites. These rocks, collectively referred to as the TTG suite, form typically relatively small (<100 to *c*. 500 km^2) and almost invariably gneissose bodies with largely concordant contact relationships with the supracrustal greenstones. These features have been explained by: (1) the diapiric ascent and emplacement of the TTGs (e.g. Viljoen & Viljoen 1969; Anhaeusser 2001); (2) the synkinematic, shallow-crustal underplating of the TTG suite at the base of the largely allochthonous and thrust greenstone

Downloaded from http://jgs.lyellcollection.org/ at Massachusetts Institute of Technology on September 17, 2019

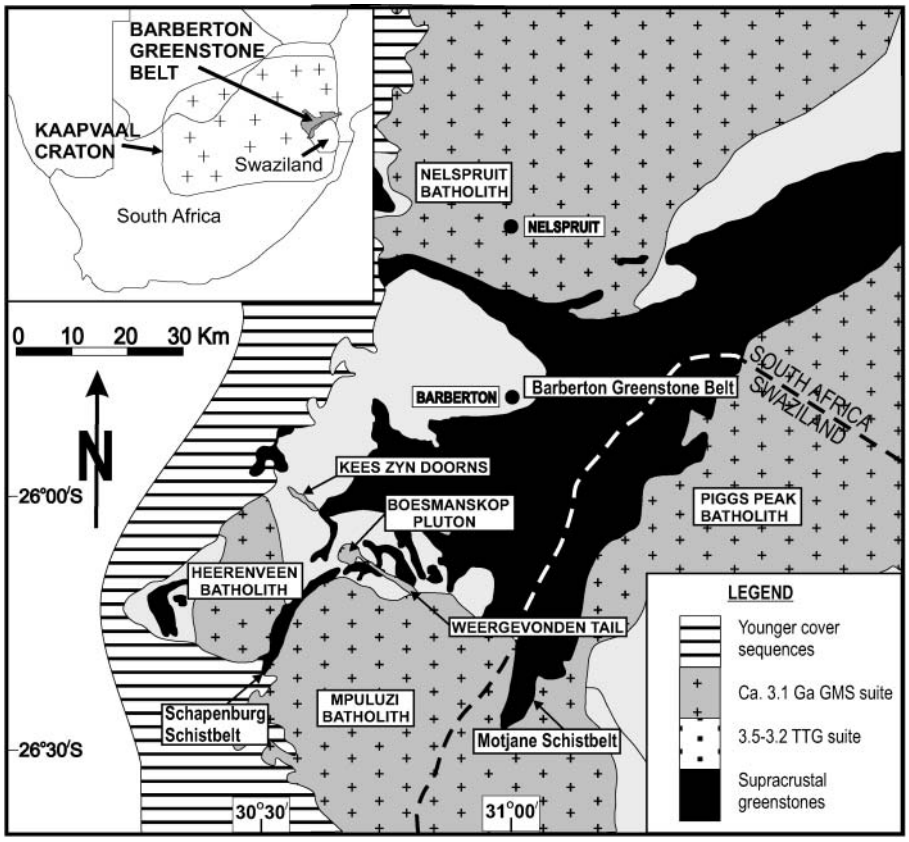

Fig. 1. Regional geology of the Barberton granite–greenstone terrane (after Anhaeusser *et al*. 1981) and its location in the Kaapvaal Craton in southern Africa (inset).

sequences (e.g. De Wit *et al*. 1987; Armstrong *et al*. 1990); or (3) questioning the magmatic models for large parts of the present-day granite–greenstone contacts altogether, as structurally reworked and subsequently exhumed basement gneisses (e.g. Dziggel *et al*. 2002; Kisters *et al*. 2003).

This study focuses on laterally extensive granite plutons of a subsequent magmatic episode associated with the intrusion of vast amounts of granodiorites, monzogranites and syenites, the GMS suite, at *c*. 3.1 Ga. Rocks of the GMS suite are found not only in the Barberton granite–greenstone terrane, but also over large parts of the Kaapvaal Craton, and their emplacement coincides with the first stabilization of the central parts of the craton (De Wit *et al*. 1992; Kamo & Davis 1994; Poujol & Anhaeusser 2001). The GMS suite in the Barberton granite–greenstone terrane shows very different internal and external characteristics from the earlier TTG suite. Individual plutons may cover several thousand square kilometres and these composite granitoid bodies have traditionally been referred to as batholiths, alluding to their compositionally and texturally heterogeneous nature and enormous areal extent (e.g. Anhaeusser *et al*. 1981). For the most part, the plutons appear undeformed, intrusion-related wall-rock strains are only locally recorded, and intrusive relationships with wall rocks are commonly sharply discordant (e.g. Hunter 1973; Anhaeusser & Robb 1983; Robb *et al*. 1983). Regional studies have demonstrated that most of these granitoids represent subhorizontal, sheet-like intrusions. The tabular granites are commonly underlain by so-called migmatite terranes and dyke complexes that have tentatively been interpreted as the feeders to the overlying granite sheets (e.g. Hunter 1957, 1973; Anhaeusser *et al*. 1981; Anhaeusser & Robb 1983; Robb *et al*. 1983). The sum of these features has traditionally been interpreted to indicate a 'passive', post-tectonic and anorogenic emplacement of the granitoids (e.g. Anhaeusser & Robb 1983). This interpretation has not remained unchallenged, and Robb *et al*. (1983) and Jackson & Robertson (1983) described the presence of regional-scale gneiss belts within and along the margins of the batholiths. The multiphase intrusive relationships between basement gneisses and the GMS suite and deformation of the potassic granitoids suggests that the emplacement of the 3.1 Ga granitoids is, at least partly, structurally controlled. As a result of these contrasting views on the contact relationships and the lack of detailed structural work on the large batholiths, the emplacement and tectonic setting of the craton-wide plutonic suite have remained somewhat enigmatic.

The present study centres around an area of *c*. 40 km × 5 km along the western and northern margin of the Mesoarchaean, *c*. 3105 Ma Mpuluzi batholith, one of the most extensively studied plutons of the GMS suite (Anhaeusser *et al*. 1981; Anhaeusser & Robb 1983; Kamo & Davis 1994; Yearron 2003) (Figs 1 and 2). The aim of this study is to constrain the emplacement mechanisms and magmatic assembly of this large batholith that combines a number of internal and external structural features that seem typical of many of the GMS suite plutons (Robb *et al*. 1983). This margin, in particular, discloses highly varying contact relationships between the younger GMS suite rocks and basement gneisses that closely reflect the existing controversy about the syn- v. post-tectonic timing and controls of the granite emplacement (Anhaeusser & Robb 1983; Jackson & Robertson 1983). Mapping was undertaken on the basis of aerial photographs at a scale of between 1:6000 and 1:10 000, and angular and spatial distortions were corrected by global positioning system (GPS) readings. The field-based studies were supplemented by thin-section petrography and whole-rock geochemistry to characterize different intrusive phases. In addition, geochronolo-

Downloaded from http://jgs.lyellcollection.org/ at Massachusetts Institute of Technology on September 17, 2019

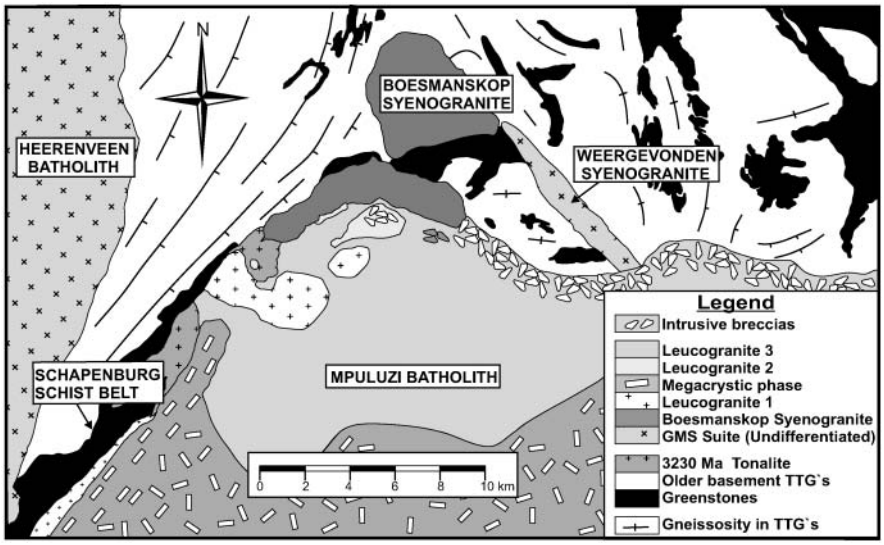

Fig. 2. Geological map of the granite–gneiss terrane south of the Barberton greenstone belt illustrating the spatial distribution of the GMS suite and older TTG gneisses and enclosed greenstone remnants.

gical results are presented on older TTG gneisses and younger potassic intrusive rocks to provide absolute age constraints on the timing of the emplacement and fabric development in different igneous phases.

The GMS suite in the study area

Rocks of the Mesoarchaean GMS suite in the area studied here include three main igneous units, namely the Mpuluzi batholith (*sensu lato*) and the smaller intrusions of the Boesmanskop and Weergevonden syenogranites situated along the NW margin of the Mpuluzi batholith (Fig. 2). The Mpuluzi batholith is a composite pluton, made up of a number of petrographically and texturally distinct phases that range in composition from granodiorite, monzonite and monzogranite to syenogranite (Anhaeusser & Robb 1983; Robb *et al*. 1983; Yearron 2003). The semicircular granitoid covers an area of at least 4000 km^2 south of the Barberton greenstone belt (Fig. 1). It occupies the high-lying peneplain between South Africa and Swaziland, and borders against the low-lying, older TTG–greenstone terrane in the north along a prominent, 500–700 m high escarpment. Its southwestern extent is concealed by younger Karoo-aged cover rocks. Other large batholiths of the GMS suite in the region include the Nelspruit batholith to the north of the Barberton greenstone belt and the Heerenveen and Piggs Peak batholith in the south and SE of the greenstone belt, respectively (Anhaeusser *et al*. 1981) (Fig. 1).

U–Pb age constraints from zircons from a fine-grained granodioritic phase indicate an age of crystallization of 3105 ± 3 Ma for the Mpuluzi granite, whereas the main, coarse-grained phase of the Boesmanskop syenogranite has been dated at 3107 +4/−2 Ma (Kamo & Davis 1994). These ages are, within error, identical to the crystallization ages of the large Nelspruit batholith (3106 ± 3 Ma), and all available age data for the GMS suite around the Barberton granite–greenstone terrane suggest a very narrow age range for the emplacement of the potassic granitoids (Kamo & Davis 1994). The *c*. 3.1 Ga age of emplacement of the GMS suite coincides with the regional D_3 phase of tectonism described from the northern parts of the Barberton greenstone belt (De Ronde & De Wit 1994). De Ronde & De Wit (1994) envisaged a transtensional tectonic environment for the D_3 tectonism. A synkinematic emplacement of the GMS suite in an extensional and rift-type tectonic setting was proposed by Kamo & Davis (1994), based on the alkaline nature of the rocks and the emplacement of some smaller plutons as NW–SE-trending, distinctly dyke-like bodies (Figs 1 and 2).

Hunter (1957, 1973) was probably the first to establish the subhorizontal, sheet-like geometry of the Mpuluzi batholith. He also estimated a thickness of the granitoid sheet of *c*. 700–1000 m based on his mapping of the Archaean granitoids in the mountaineous terrain of Swaziland. The tabular geometry has since been confirmed in regional field studies by Anhaeusser (1980) and Anhaeusser & Robb (1983), who also suggested a very shallow crustal level of emplacement for the Mpuluzi batholith mainly on the grounds of textural evidence in the granitoids. The lower- to sub-greenschist-facies metamorphic conditions of the Barberton greenstone belt to the immediate north render such shallow emplacement levels likely. However, there are, as yet, no direct and reliable *P*–*T* data that could constrain the emplacement depth.

The Mpuluzi batholith intrudes into older, *c*. 3.2–3.5 Ga, amphibolite-facies, steeply dipping, banded TTG gneisses and enclosed supracrustal greenstone remnants. Basement gneisses are parallel to the western, strongly gneissose margin of the Mpuluzi batholith (Figs 2 and 3) and structural evidence points to the rotation of the wall-rock gneissosities into parallelism with this western margin (see below). Notably, a similar belt of subvertical, NE–SW-trending gneisses within and adjacent to the Mpuluzi batholith has been described by Jackson & Robertson (1983) some 30 km SE of the present study area (Fig. 1). Here, the granites of the Mpuluzi batholith have intruded the southernmost parts of the Barberton greenstone belt, the Motjane schist belt, and both greenstones and granites have been coaxially deformed. TTG gneisses and greenstones along the northern contact of the Mpuluzi batholith are, in contrast, commonly sharply truncated by the intrusive granites (Fig. 2). The roof rocks of the Mpuluzi batholith are nowhere exposed.

Distribution of the GMS suite in the study area

The petrographic and geochemical details of the GMS suite have been given by Anhaeusser & Robb (1983), Anhaeusser (1980) and Yearron (2003). Intrusive relationships and the salient petrographic characteristics of the GMS suite are listed in

Downloaded from http://jgs.lyellcollection.org/ at Massachusetts Institute of Technology on September 17, 2019

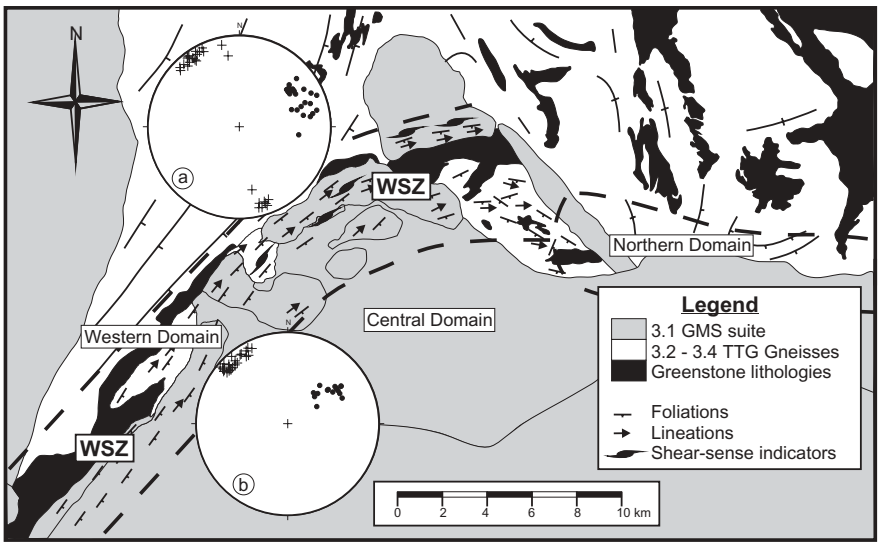

Fig. 3. Structural map of the granite–greenstone terrane south of the Barberton greenstone belt. Lower hemisphere, equal-area projections represent poles to the gneissosity (+) and mineral stretching lineations for the northern (inset a) and southern (inset b) parts of the Welverdiend shear zone (WSZ). The width of the Welverdiend shear zone is indicated by the presence of pervasive solid-state gneissosities.

Table 1. Anhaeusser & Robb (1983) used the term Boesmanskop Syenogranite Complex to describe a suite of mineralogically and texturally distinct rocks that range in composition from monzogranite to syenite. The main outcrops of this rock suite underlie the two steep-sided hills of the Boesmanskop to the immediate north of the main escarpment. The rocks at this locality are syenites, quartz syenites and syenogranites, and are typically reddish to pinkish in colour owing to their high K-feldspar content. They show medium- to coarse-grained cumulate-like textures made up of millimetre-sized, euhedral K-feldspar crystals with interstitial hornblende and/or biotite. Euhedral, millimetre-sized crystals of titanite are locally abundant. Similar rocks in the region are found only in the dyke-like Kees Zyn Doorns syenite, some 8 km to the NW (Fig. 1). The southern margin of the Boesmanskop syenogranite is deformed. This margin contains a strong NE–SW-trending solid-state gneissosity

Table 1. *Summary of the main rock types of the GMS suite, their occurrence and relative age relationships in the study area*

Main rock units	Petrography and appearance	Occurrence	Evidence for age
(9) Fourth leucogranite	Medium grey, very fine-grained, K-feldspar, plagioclase, quartz, minor hornblende, biotite and muscovite	Subhorizontal sheets in the interior of the pluton	Undeformed, crosscuts phases related to (8)
(8) Third leucogranite	Pinkish white; fine- to medium-grained; K-feldspar, plagioclase, quartz, minor biotite and muscovite	Undeformed leucogranites and large pegmatite bodies. Dominant phase along the northern margin	Contains enclaves of (1), (5) and (7)
(7) Second leucogranite	Light grey, fine-grained; K-feldspar, plagioclase, quartz, minor hornblende, biotite and muscovite	In two localities along the Welverdiend shear zone, but mainly in central domain	Weak solid-state gneissosity; intrudes (1)–(5)
(6) Weergevonden syenogranite	Light grey, fine- to medium-grained; K-feldspar, quartz, plagioclase	Weergevonden tail	No direct intrusive relationships with other phases of the GMS, locally lineated
(5) Granodiorite dykes	Medium to dark grey, fine-grained; biotite, K-feldspar, plagioclase, quartz	As NE–SW-trending dykes throughout the Welverdiend shear zone	Solid-state mylonitic fabrics, intrusive into (1), (2) and (3), no clear relationship with (4)
(4) Augengneiss dykes	Dark to medium grey with elongated, whitish pink K-feldspar augen (up to 3 cm); biotite–hornblende–feldspar–quartz groundmass	Intrusive into the northern strike extent of the Welverdiend shear zone	Solid-state gneissosity, intrusive into (1), (2) and (3), no clear relationship with (5)
(3) Megacrystic phase	Light grey to pinkish, medium- to coarse-grained, K-feldspar megacrysts (up to 5 cm), K-feldspar, plagioclase, quartz, muscovite groundmass	Mainly in the south in central domain	Locally cut by (5), contains xenoliths of (1) and (2); solid-state gneissosity along Welverdiend shear zone; local magmatic fabric
(2) First leucogranite	Light grey to pinkish grey, medium- to coarse-grained; K-feldspar, plagioclase, quartz, minor hornblende, biotite and muscovite	Lit-par-lit intrusive relationships with basement and syenogranite gneisses (1) along the Welverdiend shear zone; large, homogeneous body in the west (Fig. 2)	Solid-state gneissosity and intruded by (3) and (5), intrusive into (1). U–Pb zircon age of 3113 ± 2.4 Ma (this study)
(1) Boesmanskop syenites and syenogranites	Reddish to pinkish, K-feldspar, hornblende, biotite, minor titanite, quartz, plagioclase; considerable textural and mineralogical variations	Boesmanskop syenogranite and western margin of the Mpuluzi batholith; contacts with basement gneisses suggest, at least in parts, a subhorizontal sheet-like geometry	In places protomylonitic; xenoliths occur in most other phases of the Mpuluzi batholith, i.e. intruded by (2) and subsequent phases

Downloaded from http://jgs.lyellcollection.org/ at Massachusetts Institute of Technology on September 17, 2019

(Fig. 3) and the gradual strain increase from undeformed syenogranites in the NW to gneissic rocks in the SE can be followed over a distance of *c*. 500 m. Our regional mapping shows large tracts along the escarpment to the south and SW of the Boesmanskop pluton to be made up of similar pink gneisses. These gneisses are connected to the main outcrop of the Boesmanskop pluton, resulting in a different outcrop pattern of the syenogranites compared with that shown on published maps (Anhaeusser *et al*. 1981) (Fig. 2). Xenoliths of the pink syenitic gneisses are found in almost every other phase of the Mpuluzi batholith, indicating that the syenites form one of the earliest phases of the GMS suite in the region.

The Weergevonden syenogranite is a NW–SE-trending dyke-like intrusion that measures *c*. 8 km × 1 km (Anhaeusser 1980) (Figs 1 and 2). The syenogranite, also referred to as the Weergevonden tail (Anhaeusser *et al*. 1983), is a leucocratic, light grey and fine- to medium-grained rock, and is texturally and mineralogically distinct from the adjacent Boesmanskop syenogranite (Anhaeusser 1980). Rocks of the Weergevonden tail lack a macroscopically visible foliation but contain, in places, a steep northerly plunging lineation. The dyke-like syenogranites sharply truncate the ENE-trending gneissosity developed in, for example, gneisses related to the Boesmanskop syenogranite and the older TTG gneisses and greenstones (see below).

The main body of the Mpuluzi batholith is made up of three major phases, including: (1) a variety of fine- to medium-grained leucogranites; (2) coarsely porphyritic and often megacrystic granites; (3) locally developed fine- to medium-grained, dark grey granodiorites (Anhaeusser & Robb 1983) (Fig. 2). Pegmatite dykes, stockworks or large, irregularly shaped pegmatite pods are ubiquitous and particularly abundant along the western margin and on the topographically high-lying areas in the central parts of the Mpuluzi batholith. The northern and western parts of the study area are dominated by a variety of fine- to medium-grained, light grey to pink–grey leucogranite bodies. The leucogranites are mainly composed of microcline, plagioclase and quartz with only minor amounts of biotite and hornblende. Leucogranites in the western parts of the Mpuluzi batholith contain almost invariably a subvertical, NE-trending solid-state gneissosity defined by flattened quartz grains and the grain-shape preferred orientation of recrystallized feldspar aggregates. The northern parts of the Mpuluzi batholith, in contrast, are underlain by fine-grained leucogranites that appear undeformed in outcrop. Xenoliths of gneissose leucogranites within the undeformed leucogranite together with intrusive relationships point to the sequential emplacement of the leucogranite phases. The southern, topographically highest parts of the Mpuluzi batholith are made up of coarsely porphyritic monzogranite characterized by abundant microcline megacrysts. Fine- to medium-grained, dark grey granodiorites are locally intrusive into the megacrystic granite, forming a common spatial association termed the 'bimodal association' by Anhaeusser & Robb (1983).

Structural domains

The NW parts of the Mpuluzi batholith studied here are subdivided into a central, western and northern domain each characterized by distinctly different strains and intrusive relationships (Figs 3 and 4).

Central domain

The central domain encompasses the high portions of the Mpuluzi granite on top of the escarpment. This domain is mainly underlain by massive and largely undeformed fine-grained leucogranite in the north grading into coarsely porphyritic granite in the south (Anhaeusser & Robb 1983). Textural variations between outcrops are common and point to the rather heterogeneous nature of the granite. Granodiorites and porphyritic granites of the 'bimodal association' (Anhaeusser & Robb 1983) typically show irregular, interfingering intrusive relationships with, in places, diffuse and gradational contacts. The predominant megacrystic phase of the Mpuluzi granite locally preserves magmatic fabrics defined by the alignment of euhedral, commonly zoned K-feldspar laths, but with little evidence of regionally consistent trends. Pegmatite and granodioritic dykes form stockworks or irregularly shaped bodies. Towards the west, the feldspar megacrysts show a preferred orientation defining a NE-trending magmatic fabric. This fabric is progressively overprinted by a pervasive high-temperature gneissosity defined by feldspar augen and quartz ribbons approaching the western domain (Figs 3 and 5a).

Western domain: the Welverdiend shear zone

The Mpuluzi batholith is bounded in the west by subvertical, NE–ENE-trending gneisses that show widespread protomylonitic textures. The high-strain fabrics are pervasively developed in both basement gneisses and greenstones as well as intrusive rocks of the younger GMS suite. Non-coaxial shear fabrics are common and this western gneiss belt is referred to as the Welverdiend shear zone (Fig. 3), based on the farm Welverdiend where shear fabrics are best developed.

The Welverdiend shear zone has an arcuate trend from NE in the south to more ENE along its northern extent (Fig. 3a). The shear zone can be traced for *c*. 25–30 km along strike and the presence of subvertical, gneissose fabrics in wall rocks and the Mpuluzi granite suggests a width of *c*. 3–5 km. Banded TTG gneisses to the west of the Welverdiend shear zone show predominantly moderate dips (30–40°), but progressively rotate and steepen into parallelism with the subvertical shear fabrics over a distance of 300–500 m (Figs 3 and 4a). Metre-scale mushroom-type interference folds are contained in the steep fabric of the Welverdiend shear zone, suggesting the pervasive refoliation and refolding of earlier fabrics and folds contained in the TTG gneisses by the shear zone. The southern extent of the shear zone is covered by younger Karoo strata. Its northern, rather abrupt termination is marked by the NW–SE-trending Weergevonden syenogranite, beyond which there is no evidence of the ENE-trending shear fabrics. Mineral stretching lineations are defined by elongated quartz and quartz–feldspar mineral aggregates as well as stretched biotite clots and are locally well developed. The lineations show shallow easterly plunges in the north becoming steeper in the south of the Welverdiend shear zone (Fig. 3b). Most granitic rocks along the Welverdiend shear zone show pervasive solid-state fabrics evidenced by the dynamic recrystallization of all mineral components (Fig. 5b). Mafic minerals such as amphibole and/or biotite form part of the protomylonitic fabrics developed in greenstones and granitoids and appear largely unaltered without signs of retrogression. These features point to deformation under amphibolite-facies conditions. Retrograde brittle–ductile shearing is locally indicated by minor chloritization and epidotization along narrow, foliation-parallel cataclastic zones.

Shear-sense indicators are abundant along the northern extent of the Welverdiend shear zone. For example, large pavements along the southern, gneissose margin of the Boesmanskop syenogranite are entirely made up of closely spaced S–C fabrics

Downloaded from http://jgs.lyellcollection.org/ at Massachusetts Institute of Technology on September 17, 2019

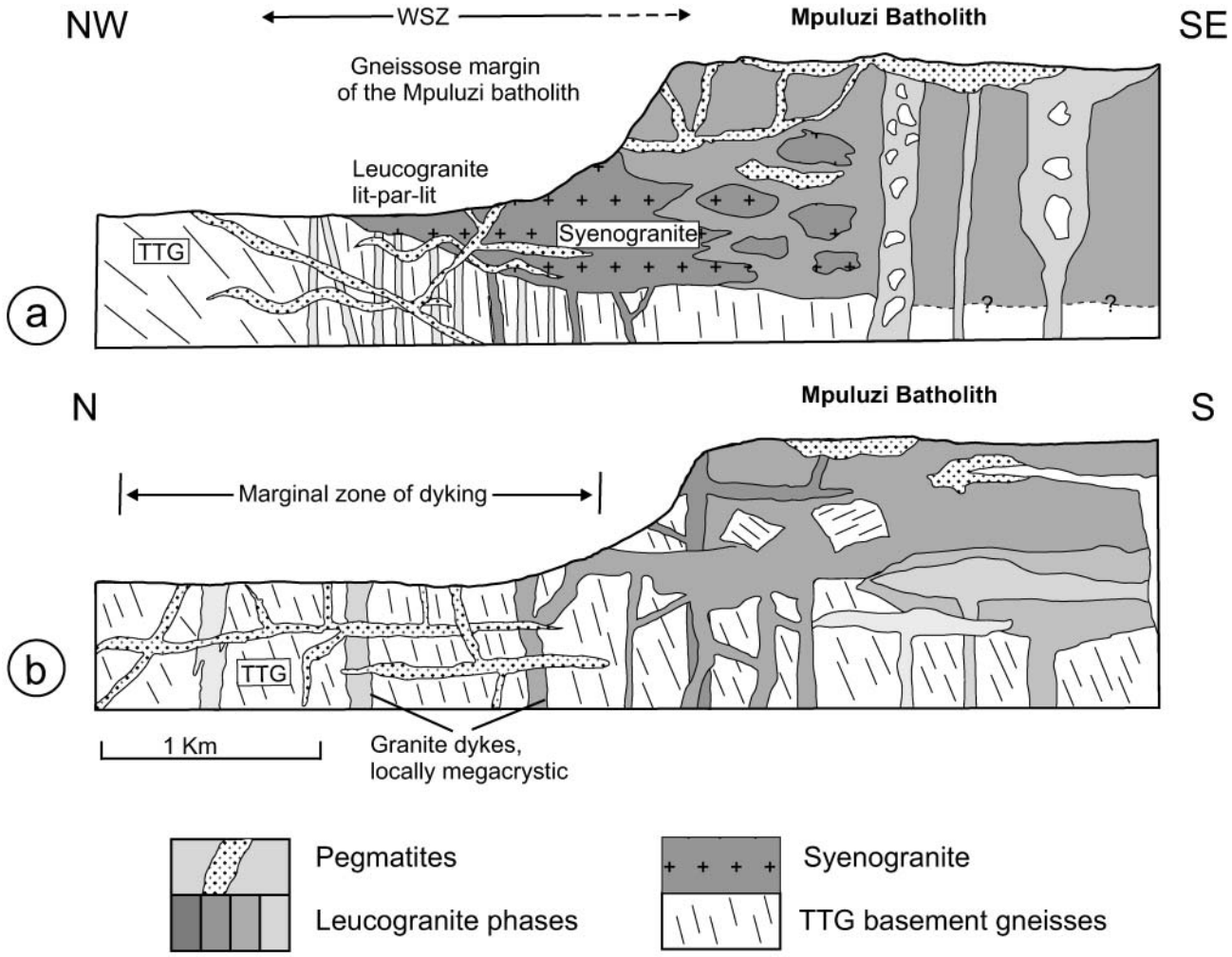

Fig. 4. Schematic cross-sections taken across the western domain (**a**) and northern domain (**b**) illustrating different intrusive relationships between rocks of the GMS suite and wall rocks (see text for detailed discussion).

Fig. 5. (**a**) K-feldspar megacrysts of the Mpuluzi batholith defining a strong NE–SW-trending fabric parallel to the western gneissose margin of the Mpuluzi batholith. At this locality (26°18.95′S, 30°56.00′E), magmatic fabrics defined by the alignment of euhedral and undeformed megacrysts are progressively overprinted by a high-*T* solid-state gneissosity approaching the western domain. The high-*T*, solid-state origin of this gneissosity is evidenced by the marginal recrystallization of megacrysts, pervasive recrystallization of the finer-grained groundmass and quartz ribbons. The top part of the photograph is made up of an intrusive leucogranite dyke that also contains a solid-state gneissosity. (**b**) Solid-state, protomylonitic gneissosity in coarse-grained (right-hand side of photo) and medium-grained (top left corner) variety of the Boesmanskop syenogranite (oblique plan view; length of pen is *c.* 15 cm). The K-feldspar megacrysts are marginally and/or pervasively recrystallized to form an augen texture and mafic minerals (biotite and hornblende) are unretrogressed. The deformation textures and mineral assemblages testify to the high-*T* origin of the protomylonitic fabric. Locality: 26°09.50′S, 30°68.95′E (Mhlingase river, SE of the Boesmanskop). (**c**) S–C fabric relationships in syenitic gneiss indicating dextral sense of shear, southern margin of the Boesmanskop syenogranite (26°06.05′S, 30°69.17′E). (**d**) Late-stage, cross-cutting and openly folded pegmatite dyke intruding into the Welverdiend shear zone (shear fabrics of the Welverdiend shear zone run approximately horizontal in the photograph). Fold axes trend NE–SW, parallel to the Welverdiend shear zone, and folding indicates a bulk NW–SE-directed shortening at high angles to the trend of the Welverdiend shear zone. Locality: 26°17.72′S, 30°57.28′E (east of the Schapenburg schist belt). (**e**) Lit-par-lit intrusive relationships between tonalitic basement gneiss (dark grey) and leucogranite veins (light grey). (Note the mylonitic fabrics and augen textures developed in the leucogranite veins.) Locality: 26°13.88′S, 30°58.62′E (foothills of the western escarpment). (**f**) Tightly folded aplite vein in syenitic gneiss. The gneissosity in the syenitic gneiss (annotated, S) is axial planar to the fold. A leucogranite dyke is intrusive into the syenitic gneiss on the right-hand side of the photograph. The leucogranite is itself strongly gneissose. Locality: 26°10.20′S, 30°62.00′E (SE margin of the Boesmanskop syenogranite). (**g**) Mosaic-like intrusive breccia of leucogranite (light grey) into a melanocratic variety of the syenogranite gneisses related to the Boesmanskop intrusion (dark grey); lens cap in upper central parts of photo for scale. Locality: 26°12.12′S, 30°61.50′E (east of the Boesmanskop syenogranite). (**h**) Intrusive breccia of weakly foliated leucogranite (light grey) containing angular fragments of foliated granodiorite (dark grey). A solid-state foliation in the leucogranite runs from the lower left-hand to the upper right-hand corner of the photograph. Locality: 26°12.83′S, 30°61.12′E (central parts of the Welverdiend shear zone).

Downloaded from http://jgs.lyellcollection.org/ at Massachusetts Institute of Technology on September 17, 2019

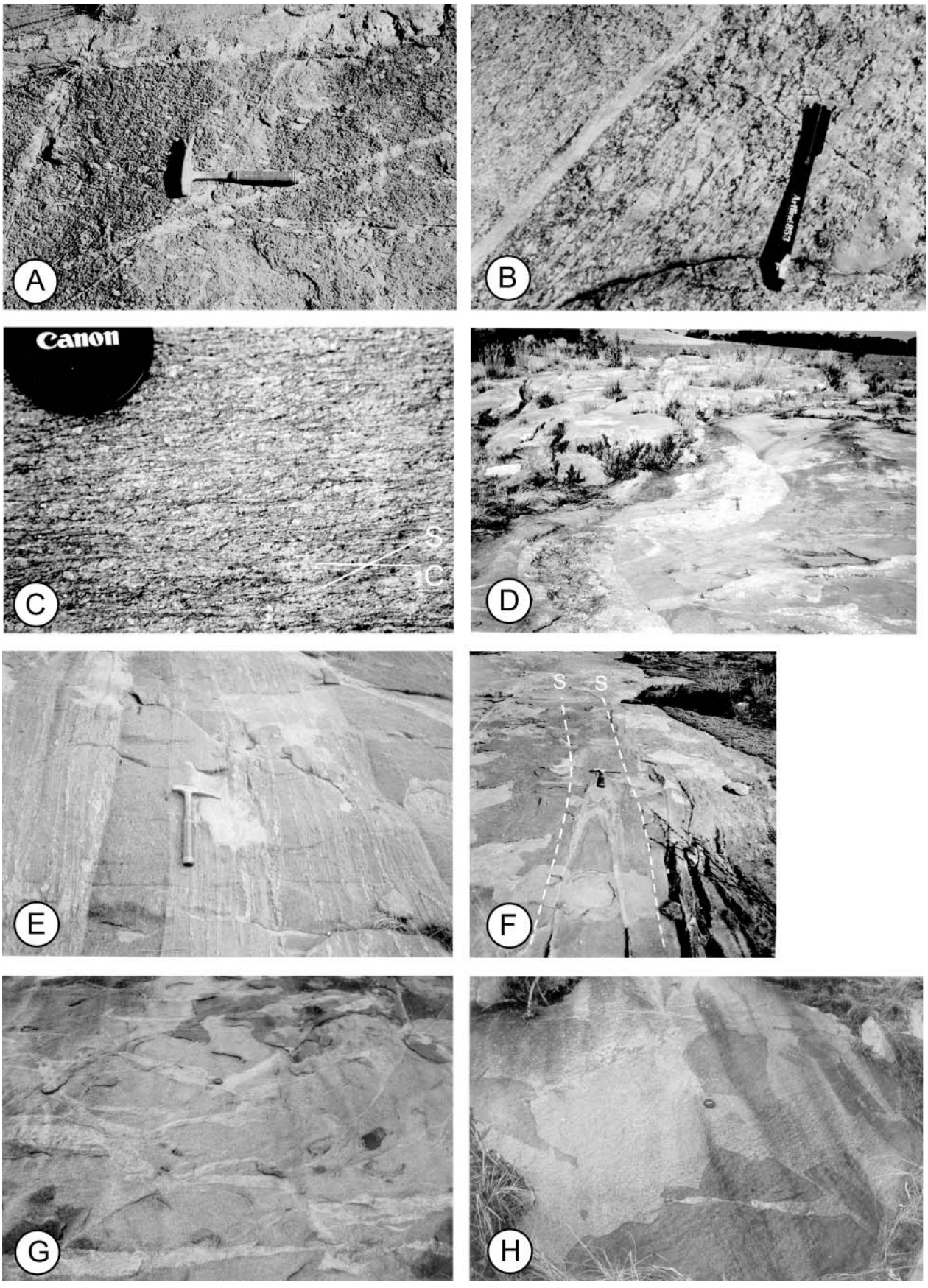

Downloaded from http://jgs.lyellcollection.org/ at Massachusetts Institute of Technology on September 17, 2019

that are pervasively developed over several tens of metres. Mica fish, and rotated σ- and δ-clasts are also present, and shear-sense indicators consistently point to a dextral sense of shear (Fig. 5c), corresponding to the shallow easterly plunge of the mineral stretching lineation. Non-coaxial shear fabrics and kinematic indicators are, in contrast, scarce along the NE-trending, southern extent of the Welverdiend shear zone. Pegmatite and leucogranite dykes that cross-cut the shear zone at high angles are openly to tightly folded into upright, symmetrical folds (Fig. 5d) and fold transposition, which is widespread along the northern extent of the Welverdiend shear zone, is rare. Granitoid sheets that have intruded subparallel to the foliation commonly show chocolate-tablet type boudinage. The fold geometries and chocolate-tablet boudinage of intrusive dykes point to a large component of NW–SE-directed subhorizontal bulk shortening perpendicular to the foliation in this southern part of the Welverdiend shear zone.

Intrusive relationships. The Welverdiend shear zone is intruded by a variety of granitoids related to the GMS suite, including leucogranites, monzogranites, granodiorites, syenogranites and quartz syenites together with abundant aplites and granite pegmatites (Table 1). Most of the granitoids form subvertical sheets that are concordant with the subvertical gneissosity in the Welverdiend shear zone; that is, they are sills or foliation-parallel and -subparallel dykes (Figs 4a and 5e, f). The subvertical granite sheets vary in width from centimetres to several tens of metres and show strike lengths of several hundred metres to kilometres. However, subhorizontal and sharply discordant sheets also occur (Fig. 4a). The subhorizontal sheets are relatively rare in the foothills of the escarpment, but become more common at higher structural levels.

Subvertical granite sheets intrude in a lit-par-lit manner (Figs 4a and 5e), parallel or at low angles to the gneissose fabric of the Welverdiend shear zone. In contrast to the assertion of Anhaeusser & Robb (1983) that the gneissose fabrics in the GMS suite represent an old fabric inherited from subsequently K-metasomatized TTG gneisses, cross-cutting relationships and the different degrees of post-emplacement deformation indicate emplacement of the various phases of the GMS suite during progressive deformation along the Welverdiend shear zone. Earlier sheets of foliation-parallel leucogranites and pegmatites are pervasively mylonitized (Fig. 5e). The intrusive granitoids show feldspar-augen textures, transposition of fabrics and large quartz ribbons that are all parallel to the external foliation of the Welverdiend shear zone. Cross-cutting dykes are folded, partly transposed or boudinaged in the gneissose foliation (Fig. 5f). Late-kinematic sheets and dykes may still preserve primary intrusive relationships such as horn-and-bridge structures, but are also typically gneissose. Late- to post-kinematic leucogranites and pegmatites are sharply discordant and cross-cut all earlier intrusions and shear-zone fabrics, forming areally extensive net-veined or stockwork-like intrusive breccias, particularly at higher levels and on top of the escarpment (Figs 4a and 5g, h).

Medium to dark grey, fine- to medium-grained granodiorites form a distinct set of subvertical NE-trending dykes. Along the escarpment, these dykes can be seen to structurally underlie the main, sheet-like Mpuluzi granite. The width of the dykes ranges from several metres to tens of metres and individual dykes can be followed vertically and along their NE strike for several hundred metres, forming a kilometre-scale anastomosing network along the eastern margin of the Welverdiend shear zone. K-feldspar, plagioclase, quartz and biotite are the main rock-forming minerals and the dykes are mineralogically and texturally similar to the fine-grained granodiorites found at structurally higher levels in the Mpuluzi granite. Within *c.* 1 km distance from the Welverdiend shear zone, granodiorite dykes commonly contain a pervasive, dyke-parallel solid-state foliation with locally abundant tight to isoclinal intrafolial folds defined by thin aplite veins. Rodding fabrics or lineated augen textures are also developed. In general, the strain intensity is commonly considerably higher in the granodiorite dykes than in the tonalitic wall-rock gneisses, which probably reflects strain localization into the dykes (e.g. Zulauf & Helferich 1997). Deeply incised river sections offer exposures east of and away from the Welverdiend shear zone into the underlying levels of the main mass of the Mpuluzi batholith. Here, the dykes may still contain a subvertical, NE-trending solid-state gneissosity, but show clear evidence of a magmatic foliation defined by clusters of aligned, elongated micrographitic and/or mafic enclaves. The trains and clusters of enclaves are parallel to the dyke walls and the solid-state gneissosity that characterizes the western margin of the Mpuluzi batholith.

Multiple sheeting and dyke-in-dyke intrusive relationships of the GMS suite rocks are common along the entire strike extent of the Welverdiend shear zone. Angular xenoliths of, for example, leucogranite gneisses in granodiorite dykes or granodioritic fragments in later leucogranites (Fig. 5g and h) commonly contain solid-state gneissosities. This demonstrates the emplacement of the GMS suite over a protracted period of time, into fully crystallized earlier intrusive rocks of the same rock suite and during regional deformation. Both the fabric orientation and fabric intensity in the intrusive dykes indicate that this deformation is related to shearing along the Welverdiend shear zone. Chilled margins are absent, suggesting the intrusion of the sheets into hot wall rocks, consistent with the inferred high-*T* conditions of deformation.

Subhorizontal or shallowly dipping granite sheets are relatively rare along the Welverdiend shear zone. Tightly folded dykes occur as well as undeformed and highly discordant sheets, which suggests the syn- to post-kinematic timing of their emplacement. Most of these sheets vary in width between *c.* 1 and 10 m. Contact relationships as well as the regional outcrop pattern suggest that the pinkish syeno-granites and syenites of the Boesmanskop syenogranite form, at least in parts, subhorizontal intrusive sheets in the western domain adjacent to the Welverdiend shear zone. The contact between the syenogranites and basement gneisses is well exposed in the river bed of the Theespruit River to the immediate NW of the escarpment and south of the Boesmanskop (Fig. 6a and b). This contact is sharp and forms a subhorizontal, slightly undulating plane along which the syenogranites sharply truncate the subvertical, banded TTG gneisses and amphibolite-facies greenstones. Dykes and veinlets of syenogranite are contained in or cross-cut the gneissosity of the underlying TTG gneisses at low angles. In numerous places the dykes can be seen to be connected to the overlying sheet-like syenogranites (Fig. 6b). The dykes and veinlets are commonly folded in the foliation of the enveloping gneisses and greenstones, and contain a variably developed solid-state foliation, indicating their synkinematic emplacement during deformation of the basement gneisses. The overlying syenogranites, however, appear massive and undeformed in outcrop.

Northern domain

The generally gneissose, NW-trending margin of the Mpuluzi batholith of the western domain shows a characteristic swing to more easterly trends at and close to the termination of the Welverdiend shear zone (Fig. 3). Beyond the shear-zone termina-

Downloaded from http://jgs.lyellcollection.org/ at Massachusetts Institute of Technology on September 17, 2019

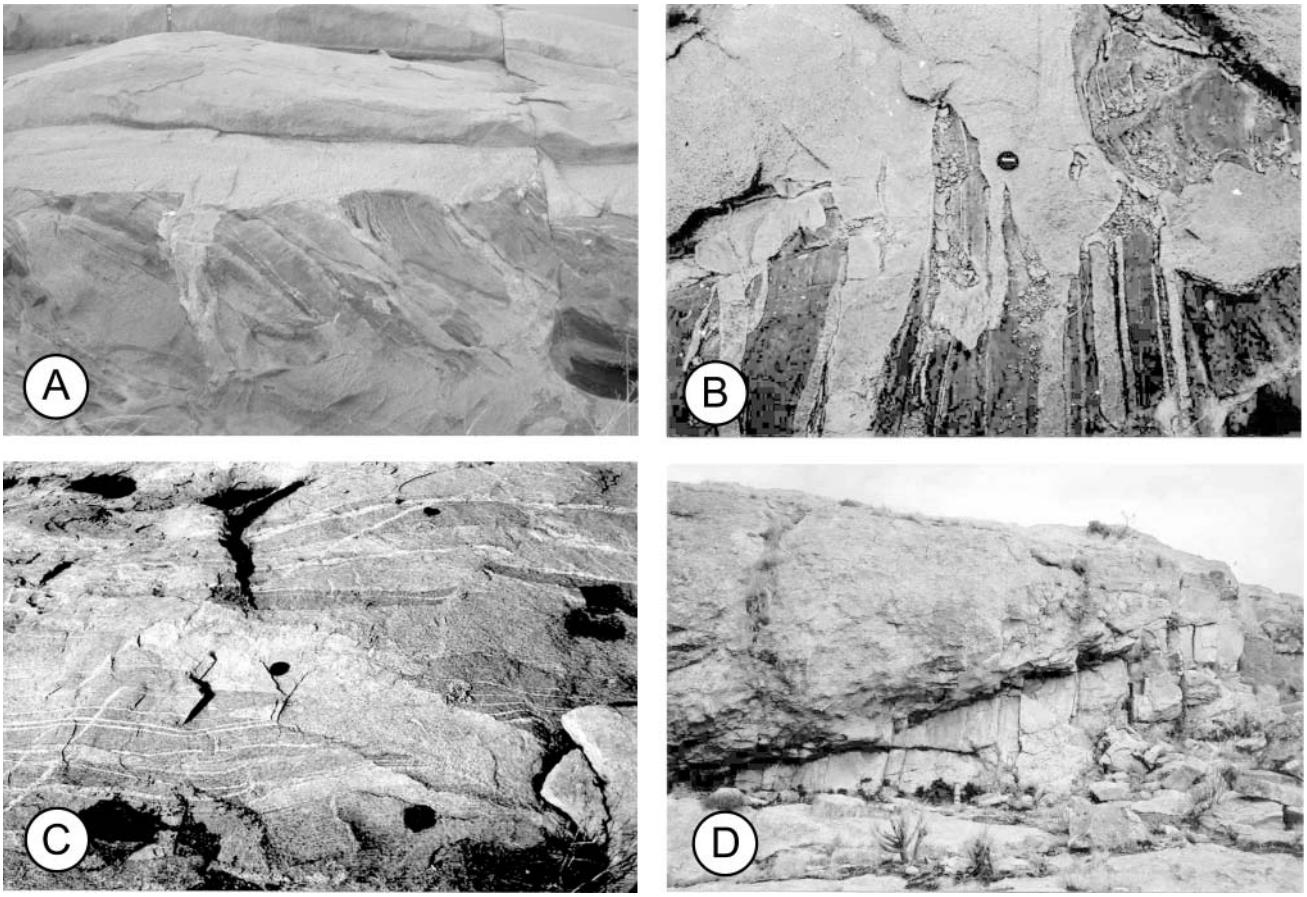

Fig. 6. (**a**) The subhorizontal contact between the syenites of the Boesmanskop pluton sharply truncating basement gneisses and amphibolites (bottom) in the Theespruit River valley to the immediate south of the Boesmanskop pluton (26°05.92′S, 30°66.28′E). (Note the undeformed dyke attached to the sheet-like syenites.) Cross-sectional view (looking SW), field of view is *c*. 1.5 m across. (**b**) Plan view of the subhorizontal eroded contact between syenites of the Boesmanskop pluton (top of the photograph) and underlying subvertical amphibolites (black) and minor TTG gneisses (dark grey) (same locality as (**a**)). The patches of syenite overlie subvertical amphibolites along a sharp subhorizontal plane. The subhorizontal sheet is connected to subvertical sheets contained within the amphibolites (bottom half of photograph). Some of the subvertical sheets are folded within the foliation of the basement (below lens cap). (**c**) Granitic dyke (light grey, centre of photograph) cross-cutting banded TTG basement gneisses in the foothills of the northern escarpment (26°06.19′S; 30°49.81′E). The dyke contains isolated K-feldspar megacrysts. (**d**) Shallowly dipping sheet of fine-grained leucogranite (central parts of the cliff) intrusive into late-stage pegmatites on top of the escarpment in the structurally higher portions of the Mpuluzi batholith in the central domain (26°12.53′S; 30°68.17′E). The cliff is *c*. 8 m high.

tion, the granites no longer intrude as mainly concordant or subconcordant sheets parallel to the Welverdiend shear zone, but rather as highly discordant dykes that cut at variable angles across the structural trend of the older TTG basement gneisses and greenstones. On a regional scale, this northern margin appears as a transition up to several kilometres wide from isolated granite dykes intrusive into TTG basement gneisses in the north, through stockwork-like intrusion breccias into the massive Mpuluzi granite of the central domain (Fig. 4b). Moreover, rocks related to the Mpuluzi batholith appear, for the most part, undeformed.

The lower levels in the northern foothills of the escarpment contain dykes of leucogranite, porphyritic granite and minor pegmatites that intrude the TTG basement gneisses (Figs 4b and 6c). The commonly discordant, subvertical granite dykes show scattered trends, but ESE-trending dykes predominate. However, most intrusive dykes contain a dyke-parallel gneissosity, which, together with the compositional similarities to the TTG basement gneisses, often complicates their recognition, and we suspect that there may be far more dykes related to the GMS suite in this region. At higher structural levels, subhorizontal sheet-like leucogranites and pegmatites become more abundant. Stockwork-like intrusive breccias result from the intersection and linkage of subhorizontal sheets with steeply dipping dykes (Fig. 4b). The dykes and sheets sharply truncate structures in the wall rock gneisses and greenstones, and large (several tens of metres) wall-rock xenoliths may be completely engulfed by the intrusive sheets. The orientation of the gneissosity in the wall-rock xenoliths commonly suggests no or very little rotation of the xenoliths with respect to the undisturbed TTG gneisses at the base of the escarpment. The continuity of structural trends from basement gneisses to large-scale basement xenoliths contained within the Mpuluzi granite preserves a ‘ghost stratigraphy’ (e.g. Pitcher 1970; Hutton 1992). A notable difference between dykes and sheets at lower structural levels and those higher up is that the latter appear undeformed. The topographically higher parts of the Mpuluzi batholith are made up of mainly massive, fine-grained leucogranite intermingled with irregular pods and dykes

Downloaded from http://jgs.lyellcollection.org/ at Massachusetts Institute of Technology on September 17, 2019

of pegmatites (Fig. 4b). However, the sheeted nature of the Mpuluzi granite is locally evidenced by subhorizontal, fine-grained leucogranite sheets that intrude and sharply truncate even late-stage pegmatites (Fig. 6d). Where exposed, both the hanging-wall and footwall contacts of the sheets are sharp. The thickness of the sheets ranges from *c*. 1.5 m (the thinnest sheets observed where footwall and hanging-wall contacts are exposed) to probably well in excess of 10 m. Xenoliths of TTG gneisses and greenstones are not as common as at lower structural levels to the north and commonly have a random orientation suggesting some degree of rotation (Fig. 4b). Xenoliths of earlier phases of the GMS suite include medium-grained leucogranite gneisses that form large bodies along the Welverdiend shear zone, and pink syenitic gneisses related to the Boesmanskop pluton.

Geochronology

U–Pb zircon and titanite ages were obtained from a tonalitic basement gneiss along the eastern margin of the Welverdiend shear zone (sample 588b) and a weakly foliated leucogranite related to the GMS suite (sample 586). These samples were analysed to confirm the *c*. 3.1 Ga age of deformation along this hitherto unrecognized shear zone and also to potentially provide estimates of the duration of the tectonism and plutonism.

U–Pb zircon and titanite ID-TIMS technique

Mineral separates were prepared from 4–6 kg rock samples. Rock samples were pulverized using a heavy-duty hydraulic rock splitter, jaw crusher and swing mill. Mineral separation involved the use of a Wilfley Table, heavy liquids (bromoform and methylene iodide) and a Frantz Isodynamic Separator.

Analyses were performed at Memorial University of Newfoundland, Canada. Normal transmitted and reflected light microscopy as well as SEM back-scattered or cathodoluminescence (CL) imagery were used to determine the zircon internal structures prior to analysis. Handpicked zircons and titanites were abraded (Krogh 1982) then washed in dilute nitric acid and ultra-pure acetone. Single grains or small populations of zircons and titanites were then placed into 0.35 ml Teflon vials together with HF and few drops of HNO_3 and a mixed ^{205}Pb–^{235}U spike. Eight of these Teflon vials were then placed in a Parr Container for several days at 210 °C (Parrish 1987). The samples were measured on a Finnigan MAT262 mass spectrometer equipped with an ion-counting secondary electron multiplier. A detailed account of the entire analytical technique has been given by Dubé *et al*. (1996).

Total Pb blanks over the period of the analyses range from 5 to 1 pg and a value of 5 pg was assigned as the laboratory blank ($^{206}Pb/^{204}Pb = 18.97 \pm 1$, $^{207}Pb/^{204}Pb = 15.73 \pm 0.5$ and $^{208}Pb/^{204}Pb = 39.19 \pm 1.5$). The calculation of common Pb was carried out by subtracting blanks and then assuming that the remaining common Pb has an Archaean composition determined from the model of Stacey & Kramers (1975). Data were reduced using PbDat (Ludwig 1993). Analytical uncertainties in Table 2 are listed at 2σ and age determinations were processed using Isoplot/Ex (Ludwig 2000).

Sample 588b: tonalitic gneiss

Sample 588b is from a medium-grained tonalitic gneiss taken to the immediate east of the Welverdiend shear zone. Zircons extracted from this sample were typically prismatic, red to yellow–whitish in colour and translucent to opaque. CL imaging revealed that they are usually concentrically and compositionally zoned without apparent core and/or rim. Five red translucent and two white–yellow grains were analysed (Table 2). The Th/U ratios vary in the range of 0.4–0.6 for the first type and 0.2–0.4 for the second. Plotted in a concordia diagram (Fig. 7a), they plot in slightly discordant to very discordant positions and do not define a simple, single group or trend, which may indicate the effects of more than one Pb-loss event. Nevertheless, we interpret this complex age pattern as follows. Four grains (Zr 1, 3, 4 and 7, Fig. 7a), define an upper intercept age of 3228 ± 12 Ma that we consider as representative of the emplacement age of this tonalite. The three remaining grains (Zr2, Zr5 and Zr6, Fig. 7a) plot above the discordia defined by the other zircons and could therefore reflect a complex Pb-loss caused by a metamorphic event and recent Pb-loss. The U–Pb zircon age of 3228 ± 12 Ma is, within error, identical to the 3231 ± 5 Ma age obtained for a gneissose tonalite some 5 km to the south in the Schapenburg schist belt (Stevens *et al*. 2002) as well as the large Kaap Valley tonalite in the north of the Barberton greenstone belt (Kamo & Davis 1994). The present mapping has also shown that the two tonalite bodies contained in the Welverdiend shear zone are probably part of a single, more extensive tonalite pluton in the southern granite–gneiss terrane (Fig. 2).

The tonalitic gneiss 588b contains a pervasive subvertical, NE-trending foliation parallel to the foliation of the Welverdiend shear zone. This raises the question of the timing of the fabric-forming event, as intrusive and structural relationships along the Welverdiend shear zone point to the *c*. 3.1 Ga intrusion of the GMS suite during high-temperature deformation. The gneissosity in the tonalite is defined by aligned hornblende and/or biotite and flattened quartz–feldspar aggregates. Titanite forms a relatively abundant accessory mineral aligned in the foliation. Five multi-fragment fractions of these titanites were analysed and data are reported in Table 2. Plotted in a concordia diagram (Fig. 7b), they plot in a concordant position, except for Sph5, and define an upper intercept age of 3124.1 ± 1.6 Ma. The four concordant titanite fractions analysed define a concordia age of 3121.9 ± 1.1 Ma that we consider as the age of crystallization of the titanite. Titanite has a high closure temperature for its U–Pb system (*c*. 630–730 °C; see Frost *et al*. 2000, for references). As the measured age of a mineral represents the age when the mineral passed through its closure temperature, this age of 3.12 Ga can be interpreted as the age of the peak of the amphibolite-facies metamorphic event and ductile deformation that affected this tonalitic gneiss.

Sample 586: Mpuluzi granite

Sample 586 represents medium-grained, greyish–pinkish leucogranite related to the Mpuluzi batholith. The granite consists of K-feldspar, plagioclase and quartz, with only minor amounts of biotite and hornblende. A gneissosity is defined by elongated quartz grains and quartz–feldspar aggregates. Zircons were prismatic, pink to reddish in colour and translucent. As for sample 588b, CL imaging of the grains is characterized by concentric magmatic zoning. Few grains show what appears to be a core surrounded by an overgrowth. Seven grains were analysed (Table 2) and plotted in a concordia diagram (Fig. 7c). Five of the seven grains (Zr1, Zr2, Zr3, Zr4 and Zr7) define an upper intercept age of 3113.2 ± 2.4 Ma. This age is suggested to represent the time of crystallization of the granite. Two points (Zr5 and Zr6) plot below this discordia in a very discordant position. Their position could be the consequence of the presence of core and overgrowth. Previous single zircon ages from undeformed potions of the GMS suite have pointed to a very narrow age range of 3105 ± 3 Ma for the entire suite (Kamo & Davis 1994). The age of the leucogranite obtained in this study is, thus, the first indication that the emplacement of the GMS

Downloaded from http://jgs.lyellcollection.org/ at Massachusetts Institute of Technology on September 17, 2019

Table 2. *Isotope dilution thermal ionization mass spectrometry U–Pb data for samples 588b (zircons and titanites) and 586 (zircons)*

Grain	Weight (μg)	U (ppm)	Pb (ppm)	Th/U	$^{206}Pb/^{204}Pb$	Radiogenic ratios						Apparent age (Ma)		
						$^{206}Pb/^{238}U$	±	$^{207}Pb/^{235}U$	±	$^{207}Pb/^{206}Pb$	±	$^{207}Pb/^{206}Pb$	$^{206}Pb/^{238}U$	Corr. coeff.
Sample 588b														
Zr 1, Pr, R, T	8	84	64	0.6	2632	0.6156	0.5	21.566	0.5	0.2541	0.08	3210	3092	0.99
Zr 2, Pr, YW, D	3	494	186	0.2	718	0.3367	0.2	9.368	0.2	0.2018	0.08	2841	1871	0.92
Zr 3, Pr, YW, D	10	191	88	0.4	1319	0.3650	1.6	11.029	1.6	0.2191	0.08	2974	2006	0.71
Zr 4, Pr, R, T	4	129	100	0.5	3799	0.6375	0.3	22.474	0.3	0.2557	0.07	3220	3179	0.97
Zr 5, Pr, R, T	7	120	80	0.5	1021	0.5580	0.3	18.821	0.3	0.2447	0.06	3150	2858	0.98
Zr 6, Pr, R, T	9	87	59	0.4	4891	0.5672	0.3	19.412	0.3	0.2482	0.14	3174	2896	0.93
Zr 7, Pr, P, T	4	59	39	0.5	875	0.5493	0.3	18.856	0.3	0.2490	0.13	3178	2822	0.94
Ti 1, 5 Fgts, R	15	57	55	2.1	141	0.6215	0.3	20.589	0.3	0.2403	0.11	3122	3116	0.93
Ti 2, 4 Fgts, R	13	46	49	2.6	124	0.6217	0.2	20.614	0.3	0.2405	0.16	3123	3117	0.84
Ti 3, 7 Fgts, R	10	80	68	1.3	114	0.6196	0.4	20.538	0.5	0.2404	0.13	3123	3108	0.96
Ti 4, 5 Fgts, R	10	60	51	1.2	92	0.6224	0.4	20.614	0.5	0.2402	0.16	3121	3119	0.94
Ti 5, 1 Fgt, R	4	186	120	0.9	382	0.4907	0.2	14.932	0.2	0.2207	0.07	2986	2574	0.95
Sample 586														
Zr 1, Pr, R, T	3	251	165	2.6	448	0.2675	0.3	6.669	0.6	0.1808	0.48	2660	1528	0.46
Zr 2, Pr, R, T	4	69	47	0.5	879	0.5658	0.5	18.319	0.5	0.2348	0.11	3085	2891	0.97
Zr 3, Pr, P, T	1	22	16	0.7	305	0.5353	0.6	17.122	0.6	0.2320	0.23	3066	2764	0.93
Zr 4, Pr, P, T	4	111	51	0.3	512	0.3961	0.4	11.665	0.4	0.2136	0.10	2933	2151	0.96
Zr 5, Pr, P, T	3	267	45	0.1	540	0.1495	0.3	3.957	0.3	0.1919	0.21	2759	898	0.84
Zr 6, Pr, P, T	3	140	41	0.4	177	0.2345	0.3	6.192	0.3	0.1915	0.17	2755	1358	0.85
Zr 7, Pr, R, T	3	27	19	0.6	567	0.5840	0.6	19.002	0.6	0.2360	0.25	3093	2965	0.91

Downloaded from http://jgs.lyellcollection.org/ at Massachusetts Institute of Technology on September 17, 2019

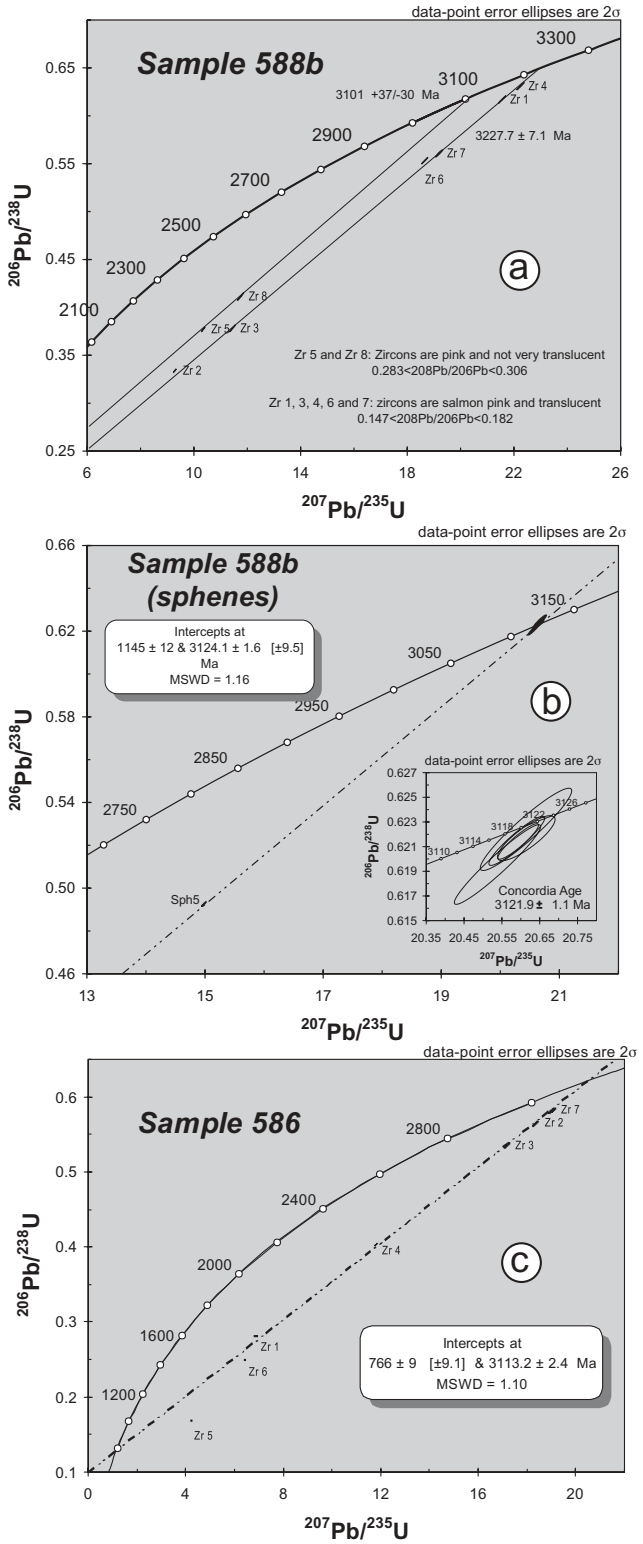

Fig. 7. U–Pb concordia diagrams for: (**a**) zircons from sample 588b, tonalitic gneiss; (**b**) titanites from sample 588b; (**c**) zircons from sample 586, leucogranite gneiss.

suite occurred over a protracted period of time and considerably longer than previously thought.

Discussion and conclusions

There are two main features that seem pertinent for an understanding of the emplacement and assembly of the Mpuluzi batholith and related phases of the GMS suite in the area. (1) The Mpuluzi batholith is bounded in the west by the synmagmatic, NE-trending dextral transcurrent Welverdiend shear zone. The termination of the Welverdiend shear zone coincides with a swing of the margin of the Mpuluzi batholith through *c*. 60° to ESE trends. Beyond the shear-zone termination, granites of the GMS suite are intruded as highly discordant sheets and appear largely undeformed. (2) The main mass of the Mpuluzi batholith is essentially made up of granite sheets, and both field and geochronological evidence point to the repeated and multiple injection of magma. Subvertical sheets and dykes dominate at lower structural levels. Higher structural levels record the rapid transition from subvertical to subhorizontal sheets that build up the main body of the tabular Mpuluzi batholith. In the following, we will address these features and their significance for the emplacement of the GMS suite in more detail.

Synkinematic emplacement of the GMS suite

The commonly observed spatial and temporal relationship between deformation and granite emplacement may be interpreted to reflect either shear-zone assisted melt transfer or strain localization related to the injection of magma along shear zones (e.g. Vauchez *et al*. 1997; Brown & Solar 1998). A distinction between the two may not always be possible. In the case of the Welverdiend shear zone, clues to the timing relationship between intrusion and deformation are potentially provided by the well-defined titanite ages from the tonalitic gneiss within the Welverdiend shear zone. Assuming that this age of 3124.1 ± 1.6 Ma represents the age of initial high-temperature deformation along the Welverdiend shear zone, then shearing has commenced well before the intrusion of the main phase of GMS magmatism at *c*. 3105 Ma. Dextral shearing along the Welverdiend shear zone is, thus, probably a manifestation of a regional deformational event and melt transport was, at least initially, controlled and assisted by the deformation. The timing of deformation coincides with the D_3 tectonism described by, for example, De Ronde & De Wit (1994) from the northern margin of the Barberton greenstone belt and confirms the contention of Jackson & Robertson (1983) of synkinematic emplacement of the Mpuluzi batholith during regional deformation. The available age data also suggest that deformation along the Welverdiend shear zone may have occurred over a period of *c*. 15 to 20 Ma, that is, between *c*. 3124.1 ± 1.6 Ma and 3105 ± 3 Ma, the younger age bracket given by the intrusion of the fine-grained, undeformed granodiorite phase dated by Kamo & Davis (1994). Progressive dextral strike-slip shearing was then, however, accompanied by the emplacement and repeated injection of the mainly foliation-parallel, concordant sheets of the GMS suite. The U–Pb zircon age of 3113 ± 2.4 Ma for a leucogranite obtained in this study is significant in this context. It illustrates episodic magma injection and the assembly of the Mpuluzi batholith between at least 3113 ± 2.4 Ma and 3105 ± 3 Ma; that is, over a period of at least 3 Ma and up to 13 Ma. The positive feedback effect between magma injection and deformation (e.g. Zulauf & Helferich 1997; Vigneresse & Tikoff 1999) is evidenced by the partitioning of strain into the intrusive sheets along the Welver-

Downloaded from http://jgs.lyellcollection.org/ at Massachusetts Institute of Technology on September 17, 2019

diend shear zone. Continued and repeated magma injection of the foliation-parallel sheets has probably resulted in higher strain rates along the Welverdiend shear zone because (1) the intrusive sheets continued to deform more easily during dyking compared with their wall rocks and (2) the wall rocks were heated during repeated granite sheeting. The latter point is illustrated by the lack of chilled margins in intrusive granite sheets and the presence of pervasive, high-temperature solid-state deformation fabrics. Both features are difficult to reconcile with the shallow level of granite emplacement proposed by previous workers without invoking the localized heating of the wall rocks.

The role of synmagmatic deformation

Magma emplacement and deformation along the western margin of the Mpuluzi batholith was controlled by the synmagmatic Welverdiend shear zone. Significantly, both intrusive relationships and strain intensity in rocks of the GMS change abruptly beyond the termination of the Welverdiend shear zone, underlining the significance of synmagmatic shearing for the emplacement of the Mpuluzi batholith as a whole. The spatial distribution of coaxial shortening fabrics in the south and non-coaxial fabrics indicating dextral strike-slip shearing along the northern extent of the Welverdiend shear zone suggests, in the simplest scenario, a principal NW–SE-directed shortening strain during regional deformation (Fig. 8). The clockwise rotation of the foliation along the northern extent of the Welverdiend shear zone is consistent with the swing of the foliation at, and close to, the termination of a dextral strike-slip shear zone. The ESE-trending margin of the Mpuluzi batholith is, thus, located in the extensional sector of the shear-zone termination. The dilational component in this area that has created space for the granites is evidenced by the 'passive' style of emplacement, the largely undeformed nature of the granites and the lack of wall-rock strains adjacent to the batholith. Similarly, both the location and orientation of the Weergevonden tail (Figs 2 and 8) correspond to an emplacement of the syeno-granites into, for example, an extensional horsetail or a normal fault at the termination of the Welverdiend shear zone. The NW–SE trend of the dyke-like Weergevonden tail and the Kees Zyn Doorns syenite is also consistent with their emplacement during regional NW–SE-directed shortening.

The regional-scale extent of the D_3 tectonism in the granite–gneiss terrane south of the Barberton greenstone belt is indicated by the synmagmatic deformation of the Mpuluzi batholith described by Jackson & Robertson (1983) from the Motjane schist belt (Fig. 1) some 30 km SE of the Welverdiend shear zone. The two gneiss belts describe an en echelon arrangement, and planar and linear fabric elements as well as the NW–SE shortening strains are similar in the Welverdiend shear zone and the eastern gneiss belt (Jackson & Robertson 1983). Jackson & Robertson (1983) did not record kinematic indicators in their early work, but given the similar structural inventory and timing of the two gneiss belts, we find it reasonable to speculate that the gneisses to the SE of the Welverdiend shear zone also record a component of dextral transcurrent shear. In this scenario, the bulk of the Mpuluzi batholith occupies a dilational jog bounded by the two NE-trending synmagmatic shear zones (Fig. 8). The ESE-trending, sharply discordant and unstrained northern margins of the Mpuluzi batholith, in contrast, attest to the intrusion of the granites into the extensional sector of the dilational jog (Fig. 8). This regional model of synmagmatic, NW-trending, en echelon shear zones and the resulting dilational jog geometry is able to reconcile the seemingly contrasting intrusive relationships

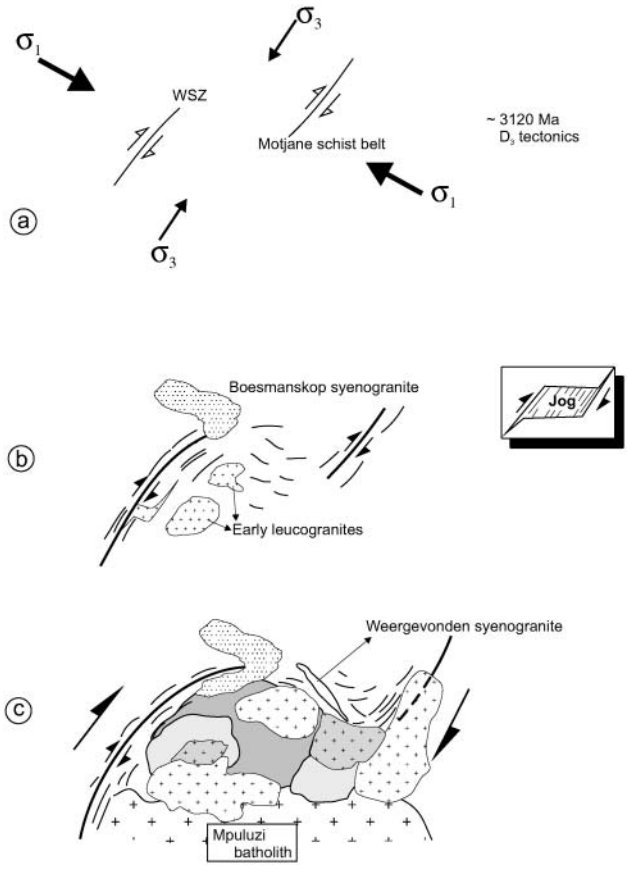

Fig. 8. Synoptic sketch of the envisaged emplacement of the Mpuluzi batholith. (**a**) Initial dextral transcurrent shearing along the Welverdiend shear zone (WSZ) and the Motjane schist belt (Jackson & Robertson 1983) during D_3-related NW–SE subhorizontal shortening. (**b**) Progressive deformation is accompanied by the emplacement of subvertical, sheet-like intrusions parallel to the shear zones, and early subhorizontal sheets such as the Boesmanskop syenogranite. The en echelon arrangement of the bounding shear zones results in a dilational jog geometry (inset). Emplacement of subvertical dykes and sheets into the dilational jog is related to progressive deformation along the bounding shear zones. (**c**) Granite sheeting continues during further deformation. The transition from subvertical dykes to subhorizontal sheets at the 'critical depth' results in the assembly of the multiphase, tabular Mpuluzi batholith. The internal assembly of the batholith is via granite sheeting; external controls are provided by regional transcurrent shearing and associated dilation.

recorded by earlier workers (Anhaeusser & Robb 1983; Jackson & Robertson 1983) as well as the arcuate map pattern of the exposed northern margin of the Mpuluzi batholith.

Assembly of the Mpuluzi batholith

One of the salient features of the Mpuluzi batholith is that it appears to be constructed of granite sheets. Regional-scale maps of the southern granite–gneiss terrane depict the close spatial relationship between granite dyking and sheeting and the perimeters of the Mpuluzi batholith in what Anhaeusser *et al*. (1981) mapped as a marginal 'migmatite belt' surrounding the granitoid. The position of the marginal migmatite belt closely corresponds to the location of the escarpment, thereby exposing the structural

Downloaded from http://jgs.lyellcollection.org/ at Massachusetts Institute of Technology on September 17, 2019

levels below the main mass of the subhorizontal Mpuluzi granite sheet. Similar intrusive relationships to those along the escarpment are exposed in deeply incised river sections that cut laterally for several kilometres into the central portions of the Mpuluzi batholith. The largest parts of the Mpuluzi batholith appear to be underlain by stockworks or swarms of multiple dyke- and sheet-like intrusions. Notably, granite dyking and sheeting is not observed in the TTG basement outside the confines of the batholith. Areas of pervasive granite sheeting are, thus, confined to regions that underwent active, synmagmatic deformation. This includes the bounding shear zones, such as the Welverdiend shear zone, and extensional sectors at either the shear-zone termination, or, on a broader scale, in dilational jogs between bounding shear zones (Fig. 8). Repeated magma injection and sheeting is probably related to slip events along the bounding Welverdiend shear zone and associated dilation. Granite sheeting into and parallel to active strike-slip shear zones such as the Welverdiend shear zone and, thus, at high angles to the bulk shortening strain is a widely documented feature (Hutton 1992; Fowler 1994). The intrusion of the foliation-parallel sheets probably tracks planes of weakness, that is, tensile strength anisotropies represented by the foliation planes in the developing shear zone (e.g. Hutton 1992). Given that large tracts of the Welverdiend shear zone are oriented at high angles to the regional NW–SE shortening strain, high magma pressures and consequently low effective pressures within the shear zone have also probably promoted transcurrent shearing along the Welverdiend shear zone. Sharply discordant granite dykes along the northern margin of the Mpuluzi batholith show scattered but predominantly ESE trends. These trends agree, at least within 20–25°, with an emplacement of the dykes into extensional fractures that opened during the NW–SE-directed regional shortening strain.

The overall intrusive pattern at lower structural levels is that of a network of relatively small-scale, interlinked magma conduits below the main, tabular Mpuluzi batholith. This network corresponds in many respects to the structurally controlled pervasive magma transfer described by Collins & Sawyer (1996). A difference is that magma transfer occurred through mainly distinct granite sheets rather than along pervasive, mainly dilational structures during ductile deformation as described by Collins & Sawyer (1996). This may reflect the relatively shallow levels of emplacement of the Mpuluzi batholith and the mainly brittle behaviour of country rocks. Brittle fracturing and sheeting probably occurred in the presence of high magma pressures and high strain rates during sheet propagation, despite the fact that wall rocks were undergoing ductile deformation during intrusion.

The intrusive features illustrated here for the Mpuluzi batholith seem to be applicable to other large batholiths in the region such as the eastern parts of the Mpuluzi batholith (Hunter 1973) and the Nelspruit batholith to the north (Robb *et al*. 1983) (Fig. 1). Notably, Robb *et al*. (1983) also described NE-trending, laterally extensive migmatite–gneiss belts for the Nelspruit batholith, but the actual structural controls probably need to be evaluated individually for each pluton.

The dyke–sheet transition

A striking feature of the Mpuluzi batholith and other batholiths of the GMS suite in the region is the rapid transition from subvertical dykes and sheets at deeper levels to subhorizontal sheets at higher structural levels. The shape and orientation of granitic sheets are determined by a variety of factors (Brisbin 1986; Hogan *et al*. 1998; Holdsworth *et al*. 1999). Some of these factors are intrinsic to the magma, including magma composition and viscosity, rate of heat loss during ascent, magma driving pressure, and the supply rate. Other factors are intrinsic to the wall rocks and include the lithostatic load, the magnitude and orientation of regional tectonic stresses, and the presence and orientation of mechanical anisotropies.

The intrusion of the Mpuluzi batholith occurred during NW–SE-directed subhorizontal shortening. Under these conditions, σ_1 and σ_3 are likely be horizontal at depth, whereas the intermediate principal stress, σ_2, is vertical. This agrees with the strike-slip kinematics recorded along the Welverdiend shear zone if a 'near-Andersonian' behaviour of the bounding shear zone is assumed. At shallower crustal levels and with a progressive decrease of the vertical load of the rock column, the least compressive stress, σ_3, will be vertical, having swapped its orientation with σ_2. This allows for the vertical dilation of the granite sheets. The depth at which this transition of the intermediate and least compressive stress occurs is sometimes referred to as the 'critical depth' (Brisbin 1986). The important consequence of the critical depth for the propagation and orientation of the granitic sheets is obvious. Subvertical granite sheets are favoured at depth, whereas subhorizontal sheets will dominate above the critical depth at shallow crustal levels. Hogan *et al*. (1998) have discussed the shape and orientation of granite sheets as a function of the relative magnitudes of magma driving pressure, lithostatic load and the presence of subhorizontal strength anisotropies in the wall rocks. The transition from subvertical dykes to subhorizontal sheet-like bodies is commonly observed to occur along subhorizontal strength anisotropies in the crust, such as the brittle–ductile transition or lithological boundaries. A prerequisite for the formation of subhorizontal granite sheets is that the magma driving pressure is sufficiently large to lift the overburden. The roof rocks of the Mpuluzi batholith are nowhere exposed, so that one can only speculate about possible rheological and/or mechanical controls of the overlying wall rocks on the emplacement and lateral spreading of the granites. Wall-rock xenoliths in the Mpuluzi batholith indicate, however, that the GMS suite intruded into banded TTG gneisses and greenstones similar to the flanking wall rocks. Given the mainly steep dips of the basement gneisses, the strength anisotropy of the wall rocks had evidently no control on the emplacement of the subhorizontal sheets of the Mpuluzi batholith. In the absence of any other obvious controls, we suggest that the transition from predominantly subvertical sheets to the subhorizontal tabular geometry of the Mpuluzi batholith tracks the location of the critical depth at the time of intrusion.

This material is based upon work supported by the National Research Foundation under grant number NRF 2053186. We greatly appreciate the co-operation of all landowners in the area during our fieldwork and thank C. Anhaeusser for sharing his regional expertise with us. J. Reavy and T. Blenkinsop are thanked for helpful reviews.

References

Anhaeusser, C.R. 1973. The evolution of the early Precambrian crust of southern Africa. *Philosophical Transactions of the Royal Society of London, Series A*, **273**, 359–388.

Anhaeusser, C.R. 1980. A geological investigation of the Archaean granite–greenstone terrane south of the Boesmanskop syenite pluton, Barberton Mountain Land. *Transactions of the Geological Society of South Africa*, **83**, 93–106.

Anhaeusser, C.R. 2001. The anatomy of an extrusive–intrusive Archaean mafic–ultramafic sequence: the Nelshoogte schist belt and Stolzburg Layered Ultramafic Complex, Barberton greenstone belt, South Africa. *South African Journal of Geology*, **104**, 167–204.

Downloaded from http://jgs.lyellcollection.org/ at Massachusetts Institute of Technology on September 17, 2019

Anhaeusser, C.R. & Robb, L.J. 1980. Regional and detailed field and geochemical studies of Archaean trondhjemite gneisses, migmatites and greenstone xenoliths in the southern part of the Barberton Mountain Land, South Africa. *Precambrian Research*, **11**, 373–397.

Anhaeusser, C.R. & Robb, L.J. 1983. Geological and geochemical characteristics of the Heerenveen and Mpuluzi batholiths south of the Barberton greenstone belt and preliminary thoughts on their petrogenesis. *In:* Anhaeusser, C.R. (ed.) *Contributions to the Geology of the Barberton Mountain Land*. Special Publication of the Geological Society of South Africa, **9**, 131–151.

Anhaeusser, C.R., Robb, L.J. & Viljoen, M.J. 1981. *Provisional geological map of the Barberton greenstone belt and surrounding terrane, eastern Transvaal and Swaziland, scale 1:250.000*. Geological Society of South Africa, Johannesburg.

Armstrong, R.A., Compston, W., De Wit, M.J. & Williams, I.S. 1990. The stratigraphy of the 3.5–3.2 Ga Barberton greenstone belt revisited: a single zircon ion microprobe study. *Earth and Planetary Science Letters*, **101**, 90–106.

Brisbin, W.C. 1986. Mechanics of pegmatite intrusion. *American Mineralogist*, **71**, 644–651.

Brown, M. & Solar, G.S. 1998. Granite ascent and emplacement during contractional deformation in convergent orogens. *Journal of Structural Geology*, **20**, 1365–1393.

Clemens, J.D., Petford, N. & Mawer, C.K. 1997. Ascent mechanisms of granitic magmas: causes and consequences. *In:* Holness, M.B. (ed.) *Deformation-enhanced Fluid Transport in the Earth's Crust and Mantle. The Mineralogical Series*. Chapman & Hall, London, 144–171.

Collins, W.J. & Sawyer, E.W. 1996. Pervasive granitoid magma transfer through the lower–middle crust during non-coaxial compressional deformation. *Journal of Metamorphic Geology*, **14**, 565–579.

Cruden, A.R. 1998. On the emplacement of tabular granites. *Journal of the Geological Society, London*, **154**, 853–862.

De Ronde, C.E.J. & De Wit, M.J. 1994. Tectonic history of the Barberton greenstone belt, South Africa: 490 million years of Archaean crustal evolution. *Tectonics*, **13**, 983–1005.

De Wit, M.J., Armstrong, R.A., Hart, R.J. & Wilson, A.H. 1987. Felsic igneous rocks within the 3.3 to 3.5 Ga Barberton greenstone belt: high crustal level equivalents of the surrounding tonalite–trondhjemite terrain emplaced during thrusting. *Tectonics*, **6**, 529–549.

De Wit, M.J., Roering, C., Hart, R.J. & Armstrong, R.A. *et al.* 1992. Formation of an Archaean continent. *Nature*, **357**, 553–562.

Dubé, B., Dunning, G.R., Lauziere, K. & Roddick, J.C. 1996. New insights into the Appalachian orogen from geology and geochronology along the Cape Ray fault zone southwest Newfoundland. *Geological Society of America Bulletin*, **108**, 101–116.

Dziggel, A., Stevens, G., Poujol, M., Anhaeusser, C.R. & Armstrong, R.A. 2002. Metamorphism of the granite–greenstone terrane south of the Barberton greenstone belt, South Africa: an insight into the tectonothermal evolution of the 'lower' portions of the Onverwacht Group. *Precambrian Research*, **114**, 221–247.

Fowler, T.J. 1994. Sheeted and bulbous pluton intrusion mechanisms of a small granitoid from southeastern Australia: implications for dyke-to-pluton transformation during emplacement. *Tectonophysics*, **234**, 197–215.

Frost, B.R., Chamberlain, K.R. & Schuhmacher, J.C. 2000. Sphene (titanite): phase relations and role as geochronometer. *Chemical Geology*, **172**, 131–148.

Guineberteau, B., Bouchez, J.-L. & Vigneresse, J.-L. 1987. The Mortagne granite pluton (France) emplaced by pull-apart along a shear zone: structural and gravimetric arguments and regional implication. *Geological Society of America Bulletin*, **90**, 763–770.

Hogan, J.P., Price, J.D. & Gilbert, M.C. 1998. Magma traps and driving pressure: consequences for pluton shape and emplacement in an extensional regime. *Journal of Structural Geology*, **20**, 1155–1168.

Holdsworth, R.E., McErlean, M.A. & Strachan, R.A. 1999. The influence of country-rock structural architecture during pluton emplacement: the Loch Loyal syenites, Scotland. *Journal of the Geological Society, London*, **156**, 163–175.

Hunter, D.R. 1957. The geology, petrology and classification of the Swaziland granites and gneisses. *Transactions of the Geological Society of South Africa*, **60**, 85–125.

Hunter, D.R. 1973. The granitic rocks of the Precambrian in Swaziland. *In:* Lister, L.A. (ed.) *Symposium on granites, gneisses and related rocks*. Special Publication of the Geological Society of South Africa, **3**, 131–145.

Hutton, D.H.W. 1988. Igneous emplacement in a shear-zone termination: the biotite granite at Strontian, Scotland. *Geological Society of America Bulletin*, **100**, 1392–1399.

Hutton, D.H.W. 1992. Granite sheeted complexes: evidence for the dyking ascent mechanism. *Transactions of the Royal Society of Edinburgh: Earth Sciences*, **83**, 377–382.

Hutton, D.H.W. & Ingram, G.M. 1992. The Great Tonalite Sill of southeastern Alaska and British Columbia: emplacement into an active contractional high angle reverse shear zone. *Transactions of the Royal Society of Edinburgh: Earth Sciences*, **83**, 383–386.

Jackson, M.P.A. & Robertson, D.I. 1983. Regional implications of Early Precambrian strains in the Onverwacht Group adjacent to the Lochiel granite, north-west Swaziland. *In:* Anhaeusser, C.R. (ed.) *Contributions to the Geology of the Barberton Mountain Land*. Special Publication of the Geological Society of South Africa, **9**, 45–62.

Jelsma, H.A., Van Der Beek, P.A. & Vinyu, M.L. 1993. Tectonic evolution of the Bindure Shamva greenstone belt (northern Zimbabwe): progressive deformation around diapiric batholiths. *Journal of Structural Geology*, **15**, 163–176.

Kamo, S.L. & Davis, D.W. 1994. Reassessment of Archaean crustal development in the Barberton Mountain Land, South Africa, based on U–Pb dating. *Tectonics*, **13**, 167–192.

Kisters, A.F.M., Stevens, G., Dziggel, A. & Armstrong, R.A. 2003. Extensional detachment faulting and core-complex formation in the southern Barberton granite–greenstone terrain, South Africa: evidence for a 3.2 Ga orogenic collapse. *Precambrian Research*, **127**, 355–378.

Krogh, T.E. 1982. Improved accuracy of U–Pb ages by the creation of more concordant systems using an air abrasion technique. *Geochimica et Cosmochimica Acta*, **46**, 617–649.

Ludwig, K.R. 1993. *A Computer Program for Processing Pb–U–Th Isotope Data, Version 1.24*. US Geological Survey, Open-File Report, **88-542**.

Ludwig, K.R. 2000. *Isoplot/Ex: a Geochronological Toolkit for Microsoft Excel*. Berkeley Geochronology Center, Berkeley, CA.

Parrish, R.R. 1987. An improved micro-capsule for zircon dissolution in U–Pb geochronology. *Chemical Geology*, **66**, 99–102.

Paterson, S.R. & Fowler, T.K. Jr 1993. Re-examining pluton emplacement mechanisms. *Journal of Structural Geology*, **15**, 191–206.

Paterson, S.R., Vernon, R.H. & Tobisch, O.T. 1989. A review of criteria for the identification of magmatic and tectonic foliations in granitoids. *Journal of Structural Geology*, **11**, 349–363.

Petford, N., Cruden, A.R., McCaffrey, K.J.W. & Vigneresse, J.-L. 2000. Granite magma formation, transport and emplacement in the Earth's crust. *Nature*, **408**, 660–673.

Pitcher, W.S. 1970. Ghost stratigraphy in granites: a review. *In:* Newall, G. & Rast, N. (eds) *Mechanisms of Igneous Intrusion*. Geological Journal Special Publication, **2**, 123–140.

Poujol, M. & Anhaeusser, C.R. 2001. The Johannesburg Dome, South Africa: new single zircon U–Pb isotopic evidence for early Archaean granite–greenstone development within the central Kaapvaal Craton. *Precambrian Research*, **108**, 139–157.

Ramsay, J.G. 1989. Emplacement kinematics of a granite diapir: the Chinamora batholith, Zimbabwe. *Journal of Structural Geology*, **11**, 191–209.

Ridley, J.R., Vearncombe, J.R. & Jelsma, H.A. 1997. Relations between greenstone belts and associated granitoids. *In:* De Wit, M.J. & Ashwal, L.D. (eds) *Greenstone Belts*. Oxford University Press, Oxford, 377–397.

Robb, L.J. & Anhaeusser, C.R. 1983. Chemical and petrogenetic characteristics of the Archaean tonalite–trondhjemite gneiss plutons in the Barberton Mountain Land. *In:* Anhaeusser, C.R. (ed.) *Contributions to the Geology of the Barberton Mountain Land*. Special Publication of the Geological Society of South Africa, **9**, 103–116.

Robb, L.J., Anhaeusser, C.R. & Van Nierop, D.A. 1983. The recognition of the Nelspruit batholith north of the Barberton greenstone belt and its significance in terms of Archaean crustal evolution. *In:* Anhaeusser, C.R. (ed.) *Contributions to the Geology of the Barberton Mountain Land*. Special Publication of the Geological Society of South Africa, **9**, 117–130.

Stacey, J.S. & Kramers, J.D. 1975. Approximation of terrestrial lead isotope evolution by a two stage model. *Earth and Planetary Science Letters*, **26**, 207–221.

Stevens, G., Droop, G.T.R., Armstrong, R.A. & Anhaeusser, C.R. 2002. The Schapenburg schist belt: amphibolite-facies metamorphism in Fig Tree Group metasediments as a consequence of c. 3.23 Ga terrane accretion in the Barberton greenstone belt, South Africa. *South African Journal of Geology*, **105**, 271–284.

Tikoff, B. & Teyssier, C. 1992. Crustal-scale, en-echelon 'P-shear' tensional bridges: a possible solution to the batholithic room problem. *Geology*, **20**, 927–930.

Van Kranendonk, M.J., Collins, W.J., Hickman, A.H. & Pawley, M.J. 2004. Critical tests of vertical vs. horizontal tectonic models for the East Pilbara Granite–Greenstone Terrain, Pilbara Craton, Western Australia. *Precambrian Research*, **131**, 173–211.

Vauchez, A., Pacheco Neves, S. & Tommasi, A. 1997. Transcurrent shear zones and magma emplacement in Neoproterozoic belts of Brazil. *In:* Bouchez, J.L., Hutton, D.H.W. & Stephens, W.E. (eds) *Granite: from Segregation of Melt to Emplacement Fabrics*. Kluwer Academic, Dordrecht, 275–294.

Downloaded from http://jgs.lyellcollection.org/ at Massachusetts Institute of Technology on September 17, 2019

Vigneresse, J.L. & Tikoff, B. 1999. Strain partitioning during partial melting and crystallizing felsic magmas. *Tectonophysics*, **312**, 117–132.

Viljoen, M.J. & Viljoen, R.P. 1969. An introduction to the geology of the Barberton granite–greenstone terrain. *In:* Haughton, S.H. (ed.) *Upper Mantle Project*. Special Publication of the Geological Society of South Africa, **2**, 9–28.

Yearron, L.M. 2003. *Archaean granite petrogenesis and implications for the evolution of the Barberton Mountain Land, South Africa*. PhD thesis, Kingston University.

Zulauf, G. & Helferich, S. 1997. Strain and strain rate in a synkinematic trondhjemite dike: evidence for melt induced strain softening during shearing (Bohemian Massif, Czech Republic). *Journal of Structural Geology*, **19**, 639–652.

Received 27 February 2004; revised typescript accepted 19 August 2004.
Scientific editing by Rob Strachan